

Supporting Information

Porous hydrogen-bonded organic-inorganic frameworks: weak interactions and selective dyes filtration

Cheng-Hui Zeng^{ab}, Zhixun Luo^{*a} and Jiannian Yao^{*a}

^a Beijing National Laboratory for Molecular Sciences (BNLMS), CAS Key Laboratory of Photochemistry, State Key Laboratory for Structural Chemistry of Unstable and Stable Species, Institute of Chemistry, Chinese Academy of Sciences, Beijing 100190, P. R. China.

E-mail: zxluo@iccas.ac.cn, jnyao@iccas.ac.cn

^b Key Laboratory of Functional Small Organic Molecule, Ministry of Education and Jiangxi's Key Laboratory of Green Chemistry, College of Chemistry and Chemical Engineering, Jiangxi Normal University, Nanchang 330022, P. R. China.

*Corresponding author, E-mail: zxluo@iccas.ac.cn, jnyao@iccas.ac.cn. Tel: +86 10 62553453, Fax: +86 10 62553453.

I. Materials and Methods

Materials

Tb₄O₇, Er₂O₃, and Y₂O₃ were purchased from non-ferrous metal materials co., LTD in Ganzhou, China. TPPZ (99%) was purchased from Aldrich Company, and it was used as received. CH₂Cl₂ and CH₃CN were purchased from Beijing Chemical Works (Beijing, China). Anodic aluminum oxide (AAO, 100 and 200 nm) were purchased from Whatman company. Deuterium oxide, deuterated nitric acid, deuterium CH₃CN and deuterium CH₂Cl₂ were purchased from Sigma-Aldrich Company.

Synthesis of HOIFs 1-3

$\text{Tb}(\text{NO}_3)_3 \cdot 6\text{H}_2\text{O}$ was prepared by dissolving Tb_4O_7 (99.9%) with concentrated HNO_3 (68%) and then evaporated at 100 °C until the crystal film formed. $\text{Er}(\text{NO}_3)_3 \cdot 6\text{H}_2\text{O}$, and $\text{Y}(\text{NO}_3)_3 \cdot 6\text{H}_2\text{O}$ were prepared with the similar method as $\text{Tb}(\text{NO}_3)_3 \cdot 6\text{H}_2\text{O}$, from Er_2O_3 (99.9%) and Y_2O_3 (99.9%), respectively. Then, 20 mL TPPZ solution (8 mM, in CH_2Cl_2) mixed with 10 mL $\text{Ln}(\text{NO}_3)_3 \cdot 6\text{H}_2\text{O}$ solution (13.7 mM, in CH_3CN). The mixture was magically stirred to react for 1 h. By controlling the evaporation speed, colorless block single crystals HOIFs **1-3** were obtained after one month.

Synthesis of d-HOIFs-1

Tb_4O_7 (99.9%, 2g) was firstly dried at 110 °C for 6 hours to exclude the water. Then, 5 mL deuterium oxide and 3 mL deuterated nitric acid were selected to react with 2 g Tb_4O_7 in 100 °C oil bath under a nitrogen atmosphere, after the Tb_4O_7 was dissolved and the solution became colorless, the solution was kept for evaporation, until the crystal film formed, the $\text{Tb}(\text{NO}_3)_3 \cdot 6\text{D}_2\text{O}$ was obtained with the yield of about 79%. Synthesis processes for **d-HOIFs-1** were similar to the procedure for **HOIFs-1**, $\text{Tb}(\text{NO}_3)_3 \cdot 6\text{D}_2\text{O}$ was dissolved in deuterium CD_3CN , to which TPPZ solution of dissolved in deuterium CD_2Cl_2 was added. The mixture was evaporated for about one month to get the **d-HOIFs-1**.

Fabrication of AAO-supported HOIFs-1 membranes

Typical a 13 mm diameter AAO disk (about 0.2 mm in thickness) was laid in a G4 sand core funnel. The G4 sand core funnel was then placed on a filter flask that connected to a vacuum pump, which was utilized to maintain a pressure differential across the AAO disk. The **HOIFs-1** solution was prepared by dissolving in a mixture solvent of CH_2Cl_2 and CH_3CN ($V_{\text{CH}_2\text{Cl}_2} : V_{\text{CH}_3\text{CN}} = 1 : 2$) to form 0.69 M **HOIFs-1** solution, then, it was added dropwise to the AAO template, and a small pressure of 0.1-0.25 MPa was maintained across the deposited film during the fabrication process. The membrane for separation dyes was fabricated with 3.5 mL volume of 0.69 M **HOIFs-1** solution dropped on the AAO template.

X-ray structure determination

Single-crystal data for HOIFs **1-3** were collected on a Bruker Smart 1000 CCD diffractometer, with Mo-K α radiation ($\lambda = 0.71073 \text{ \AA}$). All empirical absorption corrections were applied with the SADABS program. The structures were solved using direct methods, which yielded the positions of all non-hydrogen atoms. These structures were refined first isotropically and then anisotropically. The disordered electron density of the heavily disordered molecules were treated as a diffuse contribution using the program SQUEEZE. All calculations of crystal structures were performed using the SHELXTL system. All the hydrogen atoms of TPPZ and $\text{Tb}(\text{NO}_3)_3 \cdot (\text{H}_2\text{O})_3$ were placed in calculated positions with fixed isotropic thermal parameters and included in the structures factor calculations in the final stage of full-matrix least-squares refinements.

First-principles calculation

In the theoretical calculation by Gaussian program package, the structure of TPPZ and HOIFs-1 were not reorganized by DFT-optimization calculation; instead, energy and orbital calculations are performed based on the original crystal structure without any constraints on the geometry. The basis set was chosen as B3LYP/6-31g level of theory for TPPZ and $\text{Tb}(\text{NO}_3)_3 \cdot (\text{H}_2\text{O})_3$, and B3LYP/6-31g/RECP level of theory for **HOIFs-1**.

Instrumentation

The morphology of the nanostructures was examined by field-emission scanning electron microscopy (SEM; Hitachi S-4800). Energy dispersive spectrometer (EDS) was measured on the same equipment. The phase purity of bulk samples was determined by X-ray diffraction (XRD), using a DMAX2200VPC diffractometer, at 30 kV and 30 mA. Luminescence spectra were recorded on a RF-5310PC (Shimadzu) Spectrofluorophotometer. The luminescence lifetime was measured on an Edinburgh FLS 920 instrument. The ^1H NMR spectra was recorded on a Bruker Advance 400 NMR spectrometer with resonance frequencies of 400 MHz in a mixed solvent of Deuterium DMSO and Deuterium CH_2Cl_2 . Thermogravimetric analysis (TGA) was recorded on a Netzsch–Bruker TG-209 unit at a heating rate of 5°C/min under atmosphere. Infrared spectra were obtained in KBr pellets and recorded on a Nicolet 330 FT-Irspectrometer in 4000-400 cm^{-1} at room temperature. Raman spectra were collected on a Bruker OPTIK GmbH RAM II at room temperature with an excitation at 1064 nm. All these

experiments were measured at 298 K. Elemental analyses (C, H O and N) were performed on an EA3000 elemental analyzer.

II. Chemical Structures

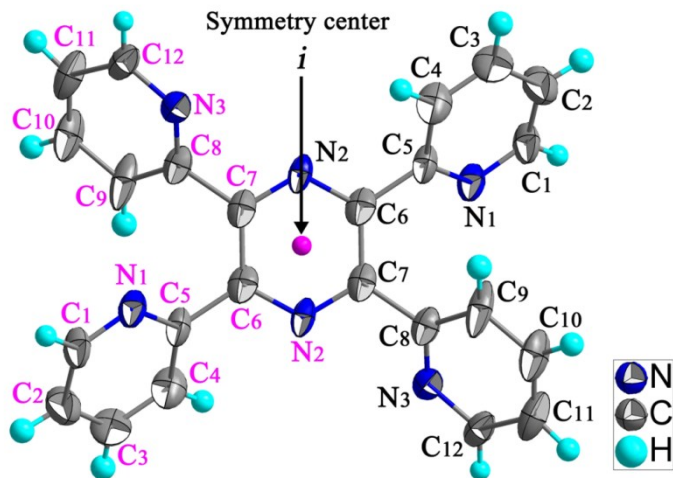


Fig. S1 The organic component TPPZ in **HOIFs-1**. It is centrosymmetric, the symmetric center is at the pyrazine ring.

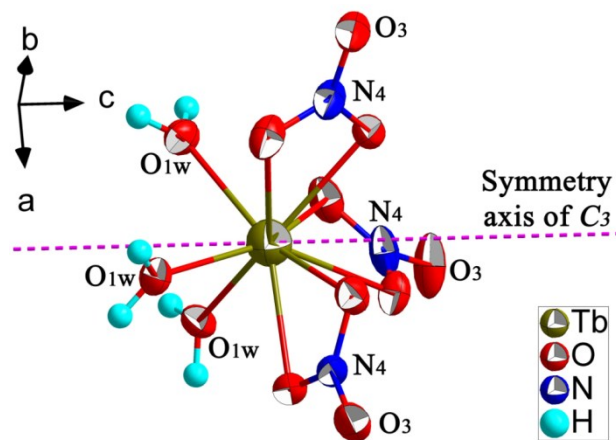


Fig. S2 The inorganic component $\text{Tb}(\text{NO}_3)_3 \cdot 6\text{H}_2\text{O}_3$. It is axisymmetric, with the symmetric axis crossing the Tb atoms and both the center of the plane formed by three NO_3^- groups and three H_2O molecules.

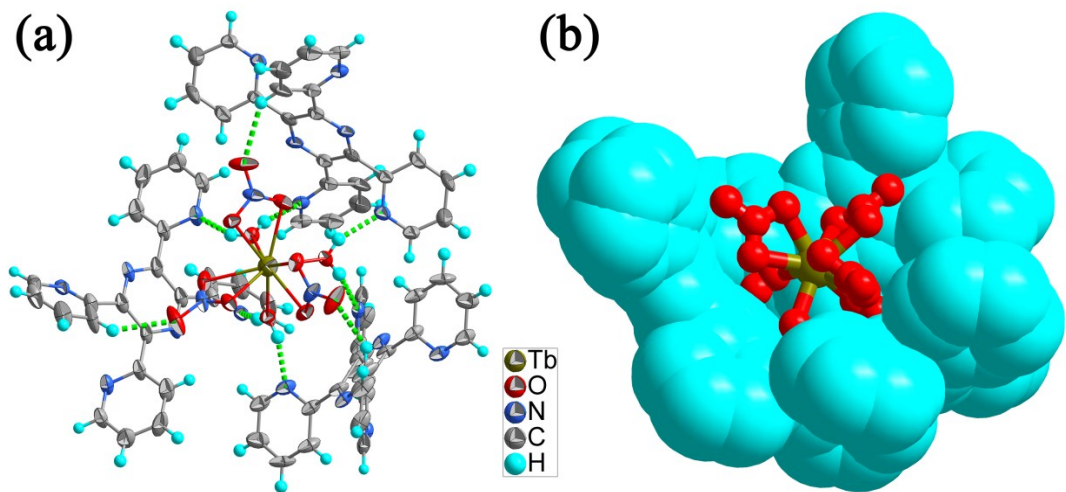


Fig. S3 The composition involving the inorganic component $\text{Tb}(\text{NO}_3)_3 \cdot 6\text{H}_2\text{O}$ and three TPPZ molecules in **HOIFs-1**. (a) Three TPPZs connect with three H_2O molecules in one $\text{Tb}(\text{NO}_3)_3 \cdot (\text{H}_2\text{O})_3$ by three $\text{O}_{1\text{W}}\text{-H}_{1\text{WA}} \cdots \text{N}_3 = 2.718 \text{ \AA}$, three $\text{O}_{1\text{W}}\text{-H}_{1\text{WB}} \cdots \text{N}_1 = 2.720 \text{ \AA}$ and three $\text{C}_9\text{-H}_9 \cdots \text{O}_3 = 3.187 \text{ \AA}$, with the DAADAADAA-ADD·ADD·ADD bond array (green dash lines: hydrogen bonds); (b) a pattern showing the pearl-in-bowl configuration of the three TPPZ and one $\text{Tb}(\text{NO}_3)_3 \cdot (\text{H}_2\text{O})_3$.

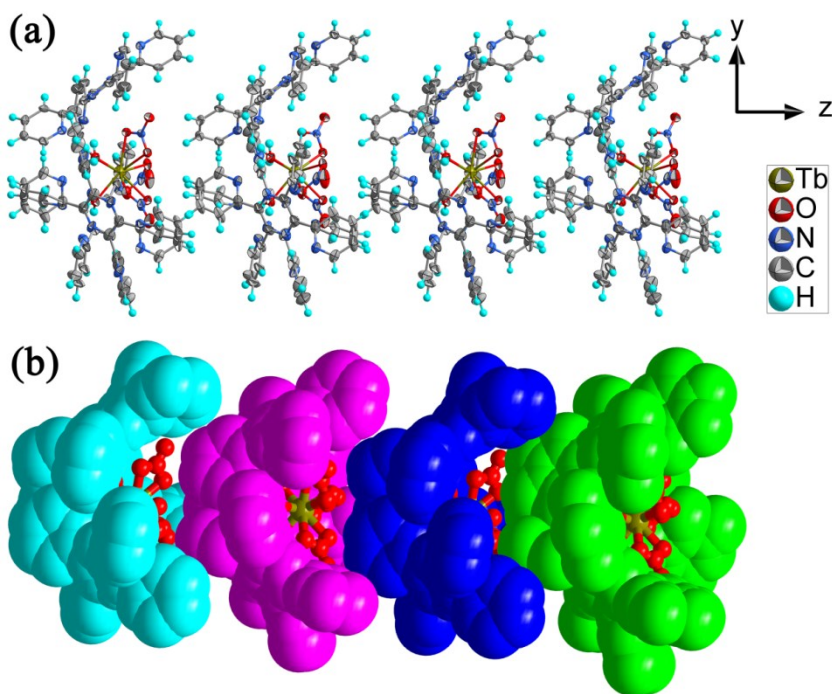


Fig. S4 The primitive accumulation form involving the pearl-in-bowl **HOIFs-1** building blocks. (a) The pearl-in-bowl unit connects with each other by van der Waals' force to form a 1D structure in the oz direction; (b) the bowl-in-bowl stacking 1D structure in the oz direction.

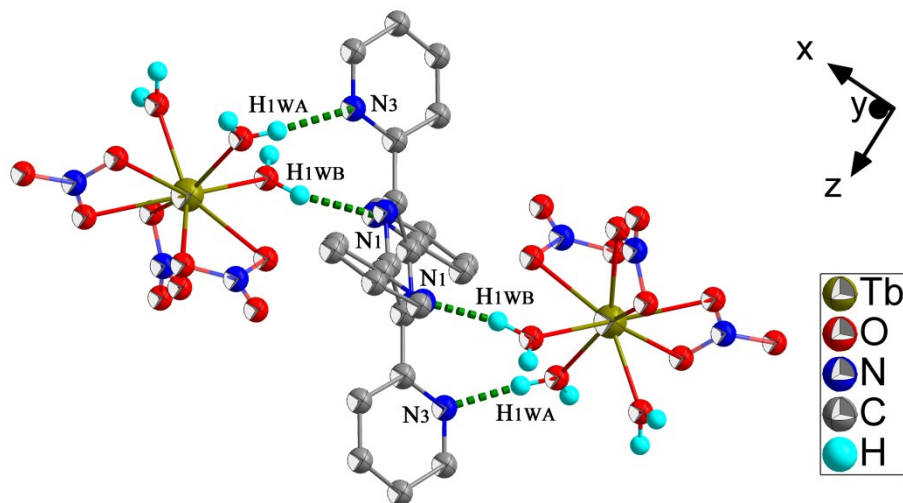


Fig. S5 The adjacent 1D bowl-in-bowl stacking structure by connecting with each other via hydrogen bonds ($\text{O}_{\text{W}}-\text{H}_{\text{WA}} \cdots \text{N}_3$ and $\text{O}_{\text{W}}-\text{H}_{\text{WB}} \cdots \text{N}_1$) to form 3D porous stacking structure.

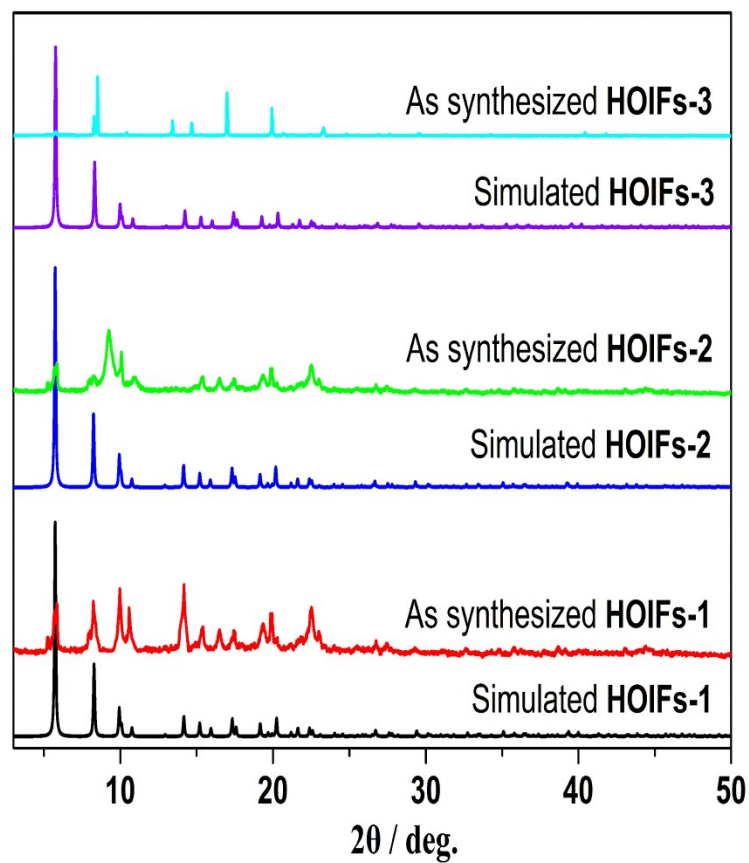


Fig. S6 XRD patterns for as synthesized HOIFs **1-3**, comparing with the simulated data.

III. IR and Raman Analysis

The C-H vibration in TPPZ is at about 3000 cm^{-1} , however, this pick broadens in HOIFs **1-3** (Fig. S7a, b), which is due to the hydrogen bond formation between N in TPPZ and H of coordination water ($\text{O}_{1w}\text{-H}_{1wa}\cdots\text{N}_3$ and $\text{O}_{1w}\text{-H}_{1wb}\cdots\text{N}_1$). The disappearance of C=C vibration on the pyridine ring at 1487, 1476 and 1435 cm^{-1} (Fig. S7c), and the missing of C=N vibration at 1123 cm^{-1} (Fig. S7b), implying the hydrogen bonds interaction of N on the pyridine ring with H. The missing of wagging vibration of C-H on the pyridine ring at 989 cm^{-1} also infers the hydrogen-bond interaction (Fig. S7b). DFT-calculation results of TPPZ, $\text{Tb}(\text{NO}_3)_3\cdot(\text{H}_2\text{O})_3$ and **HOIFs-1** also indicate two new peaks at 920 and 1480 cm^{-1} of the IR spectra, further confirming the hydrogen bonds interaction of TPPZ and $\text{Tb}(\text{NO}_3)_3\cdot(\text{H}_2\text{O})_3$ (Fig. S7d).

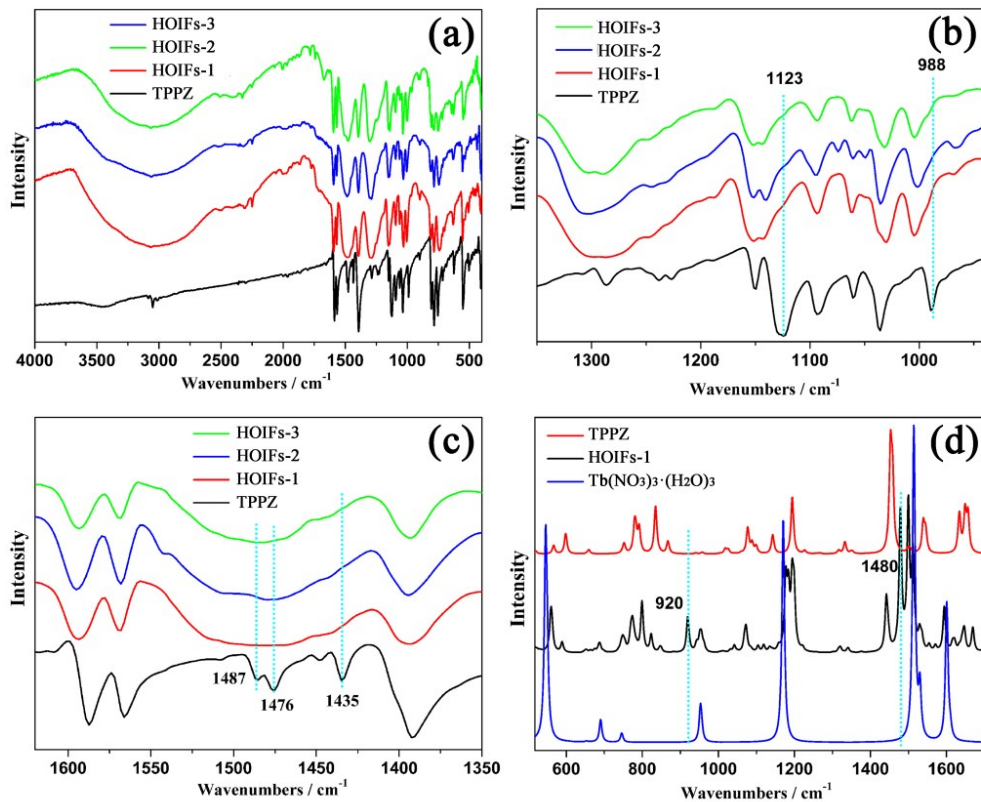


Fig. S7 a) IR spectra of TPPZ and HOIFs **1-3**; b) and c) are enlargement of a); d) DFT-calculation of TPPZ, $\text{Tb}(\text{NO}_3)_3\cdot(\text{H}_2\text{O})_3$ and **HOIFs-1**.

Fig. S8a shows the IR spectra of **HOIFs-1**, where the calculated results coincide with the experimental spectrum. **Fig. S8b** provides a comparison of experimental IR spectra for HOIFs **1-3** and TPPZ. The significant similarity of HOIFs **1-3** is due to their identical chemical structure. It is also notable that the three peaks of 1124 (C-H wagging), 1476 and 1485 cm⁻¹ (C=C stretching) of TPPZ disappear in the spectra of HOIFs 1-3, along with the emergence of a new peak at 966 cm⁻¹ (stretching vibration of N=O) emerges, owing to the weak interactions with Tb(NO₃)₃·(H₂O)₃. This diversity also can be seen in experimental Raman results (**Fig. S8e**), where two Raman peaks in TPPZ at 2987 and 2937 cm⁻¹ weakened, while 3054 and 992 cm⁻¹ are bathochromic-shifted to 3072 and 1002 cm⁻¹, respectively. Also DFT calculated IR activities find two new peaks at 920 and 1480 cm⁻¹ (**Fig. S8c**). The calculated Raman result shows that the 1632 cm⁻¹ mode (C=C stretching vibration) in TPPZ splits into two peaks (**Fig. S8f**) after it interacts with Tb(NO₃)₃·(H₂O)₃ by hydrogen bond. All these experimental and DFT-calculation results reveal the dominant hydrogen-bonds interactions between TPPZ and Tb(NO₃)₃·(H₂O)₃ in HOIFs **1-3**. More detailed analysis can be seen in **Table S14**.

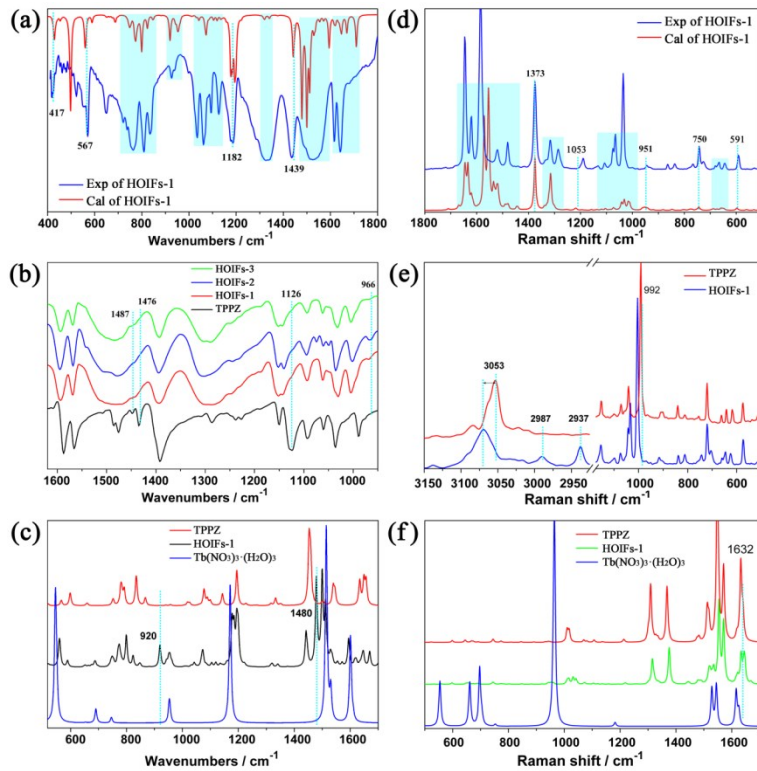


Fig. S8 (a) Experimental and calculated IR spectra of **HOIFs-1**. (b) A comparison of experimental IR spectra for HOIFs **1-3** and TPPZ; (c) comparison of calculated IR spectra for TPPZ, **HOIFs-1** and Tb(NO₃)₃·(H₂O)₃; (d) comparison of experimental and calculated Raman spectra of **HOIFs-1**; (e) comparison of experimental Raman spectra of TPPZ and **HOIFs-1**; (f) comparison of calculated Raman spectra for TPPZ, **HOIFs-1** and Tb(NO₃)₃·(H₂O)₃.

IV. UV-vis and luminescence analysis

Fig. S9a shows the UV-vis absorption spectra of TPPZ and **HOIFs-1**. It is notable that the n- π^* absorption bands of C=C and C=N in TPPZ (at 277 and 312 nm, respectively) take on bathochromic-shifts (at 293 and 335 nm, respectively), and a new shoulder peak appears at \sim 362 nm pertaining to the hydrogen bonds interactions between TPPZ and $\text{Tb}(\text{NO}_3)_3 \cdot (\text{H}_2\text{O})_3$. Interactions of TPPZ and $\text{Tb}(\text{NO}_3)_3 \cdot (\text{H}_2\text{O})_3$ also induce fluorescence quench of TPPZ (excited at 445 nm, Fig. S9b), where TPPZ solution is luminescent and has a single-exponential decay lifetime of 2.75 ns (monitored at 505 nm, inset of Fig. S9b). The fluorescence quench is largely due to the charge transfer (CT) from TPPZ to $\text{Tb}(\text{NO}_3)_3 \cdot (\text{H}_2\text{O})_3$, and the CT will be further confirmed hereinafter on a basis of DFT-calculation results.

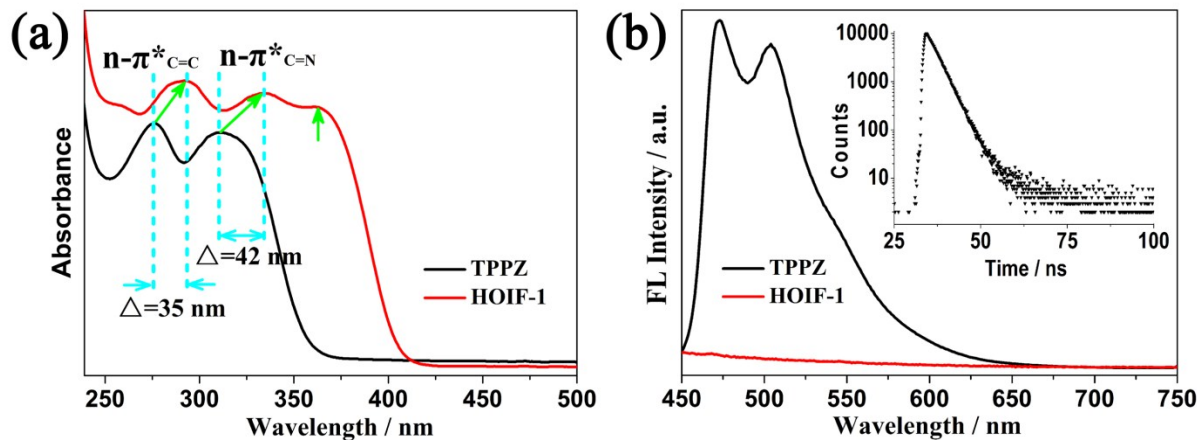


Fig. S9 (a) UV-vis of TPPZ (8.2 mM, in CH_2Cl_2) and **HOIFs-1** (0.55 mM, in $\text{V}_{\text{CH}_2\text{Cl}_2} : \text{V}_{\text{CH}_3\text{CN}} = 1 : 2$) at 298 K; (b) fluorescence ($\lambda_{\text{ex}} = 445$ nm) of TPPZ (8.2 mM, in CH_2Cl_2) and **HOIFs-1** (0.55 mM, in $\text{V}_{\text{CH}_2\text{Cl}_2} : \text{V}_{\text{CH}_3\text{CN}} = 1 : 2$) at 298 K. Inset: fluorescence decay lifetime of TPPZ monitored at 505 nm;

V. Deuterated Experiments

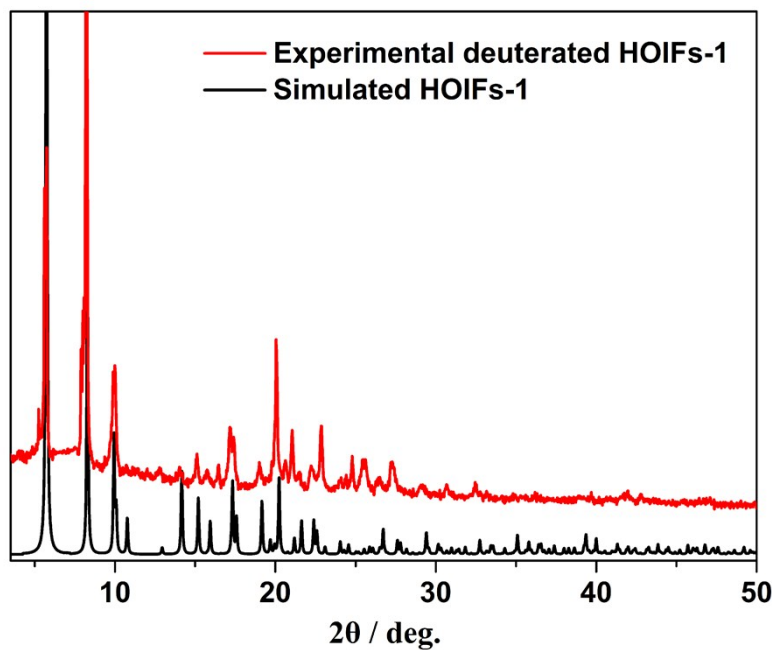


Fig. S10 PXRD comparision of simulated **HOIFs-1** and **d-HOIFs-1**.

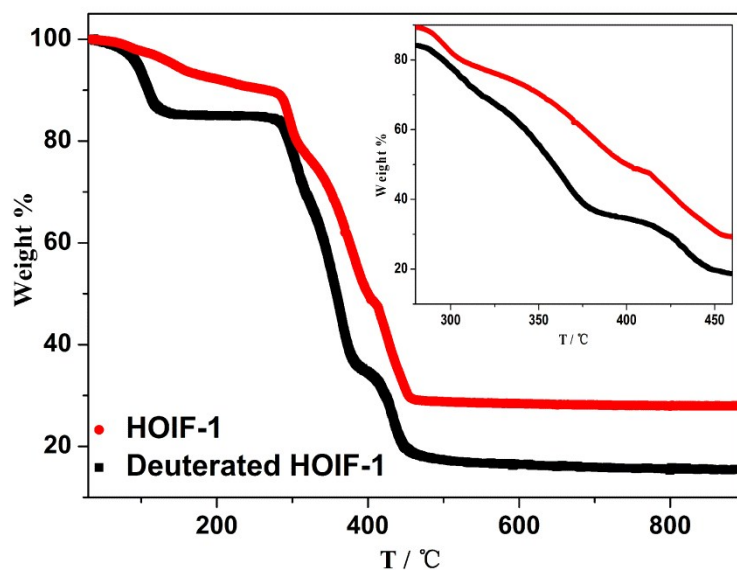


Fig. S11 TGA of **HOIFs-1** and **d-HOIFs-1** measured under atmosphere, (Inset) the framework collapsion of **HOIFs-1** is more quick than **d-HOIFs-1**, to confirm the hydrogen bonds functions the thermal stability of **HOIFs-1**.

VI. Orbital Analysis

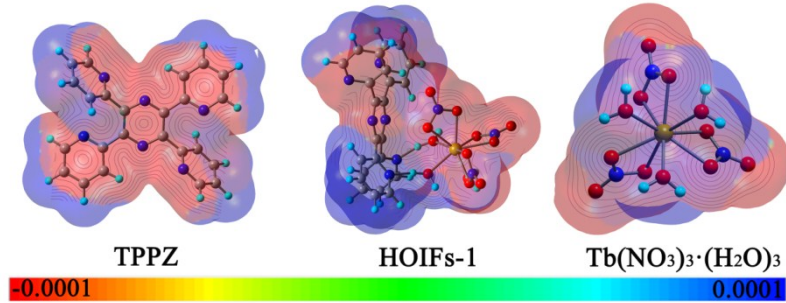


Fig. S12 Molecular electrostatic potential surfaces of the species TPPZ, **HOIFs-1** and $\text{Tb}(\text{NO}_3)_3 \cdot (\text{H}_2\text{O})_3$, respectively, (the isodensity contours are 0.0002 electron per bohr), the negative and positive isovalues surfaces are given in blue and red mapping, respectively, maxima and minima correspond to ± 0.0001 au.

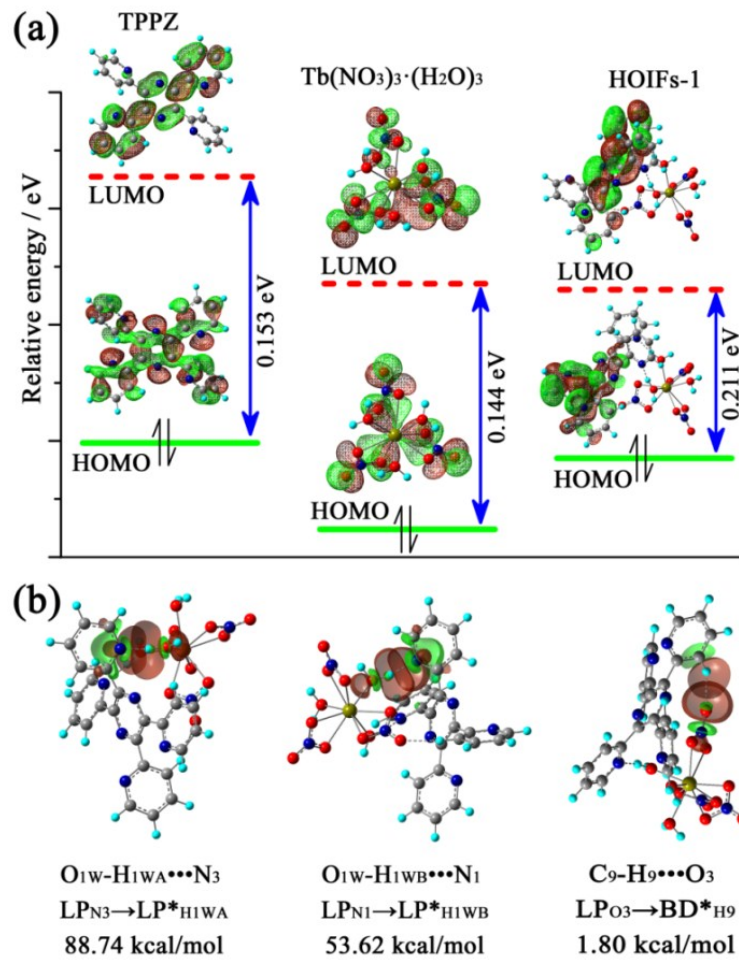


Fig. S13 (a) The HOMOs, LUMOs, and HOMO-LUMO gaps of TPPZ, **HOIFs-1** and $\text{Tb}(\text{NO}_3)_3 \cdot (\text{H}_2\text{O})_3$, the HOMOs and LUMOs are indicated by green solid lines and red dash lines, respectively. (b) NBO donor-acceptor (overlap) interactions of $\text{O}_{1\text{W}}-\text{H}_{1\text{WA}} \cdots \text{N}_3$, $\text{O}_{1\text{W}}-\text{H}_{1\text{WB}} \cdots \text{N}_1$ and $\text{C}_9-\text{H}_9 \cdots \text{O}_3$ in **HOIFs-1**. The positive donor orbitals are green and negative donor orbitals are brownish red, respectively.

VII. Morphologic Analysis

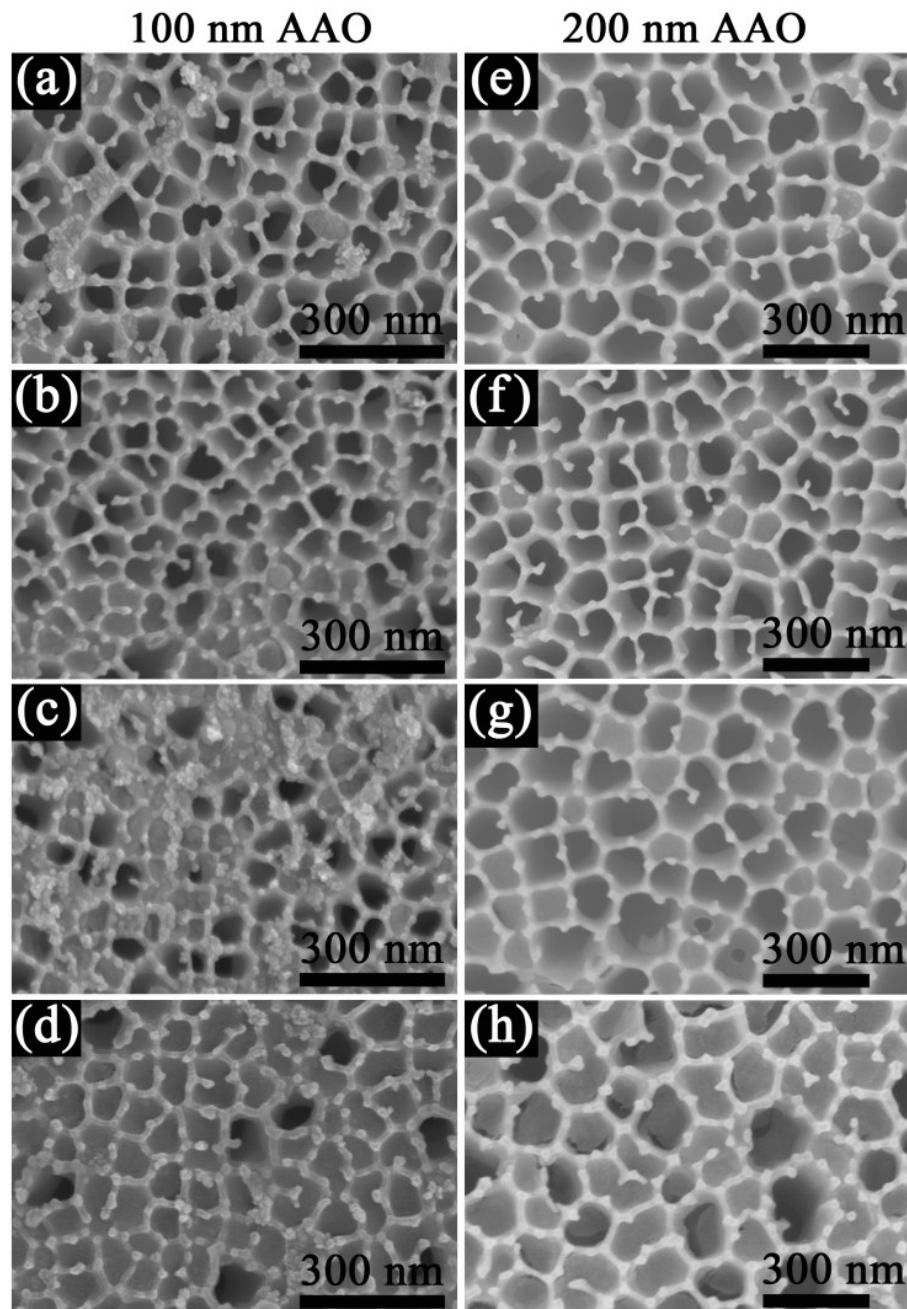


Fig. S14 SEM images of AAO-supported HOIF1. (a-d): the pores blocked step by step with the solution addition to the 100 nm AAO from 0.2 to 0.8 mL 0.69 M **HOIFs-1** solution (a: 0.2 mL; b: 0.4 mL; c: 0.6 mL; d: 0.8 mL); (e-h): the pores blocked step by step with the solution addition to the 200 nm AAO from 0.2 to 0.8 mL 0.69 M **HOIFs-1** solution (e: 0.2 mL; f: 0.4 mL; g: 0.6 mL; h: 0.8 mL).

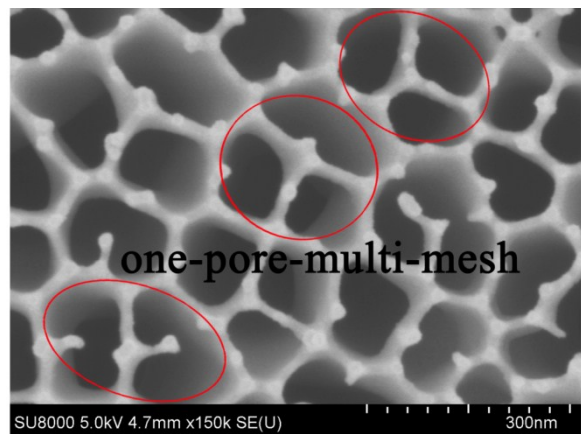


Fig. S15 One-pore-multi-mesh mode of porous **HOIFs-1** membrane on the AAO.

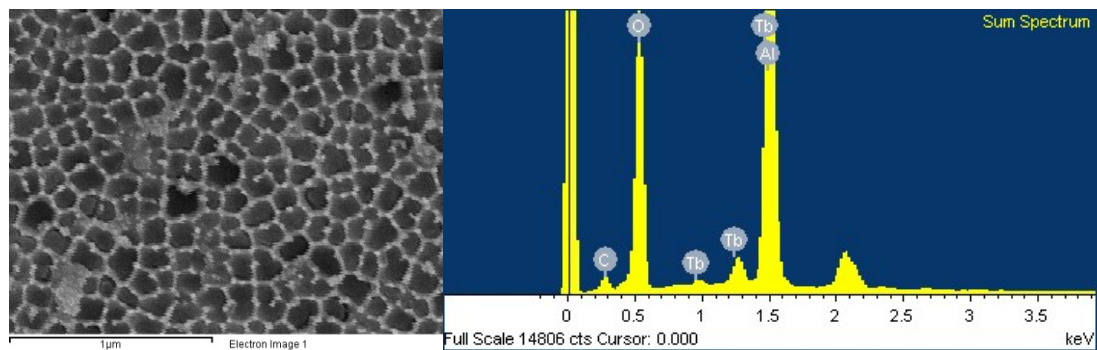


Fig. S16 EDS of the **HOIFs-1** membrane, C and Tb come from the organic and inorganic component of **HOIFs-1**, respectively, Al and most of the O are ascribed to the template of AAO.

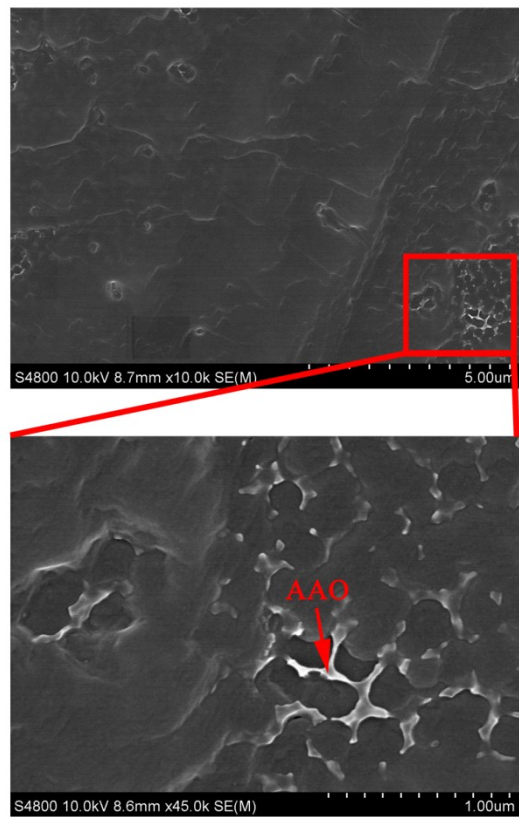


Fig. S17 SEM of 3.5 mL **HOIFs-1** solution dropped on 100 nm AAO, SEM shows the **HOIFs-1** membrane on the AAO is plat and compact, and the holes are blocked.

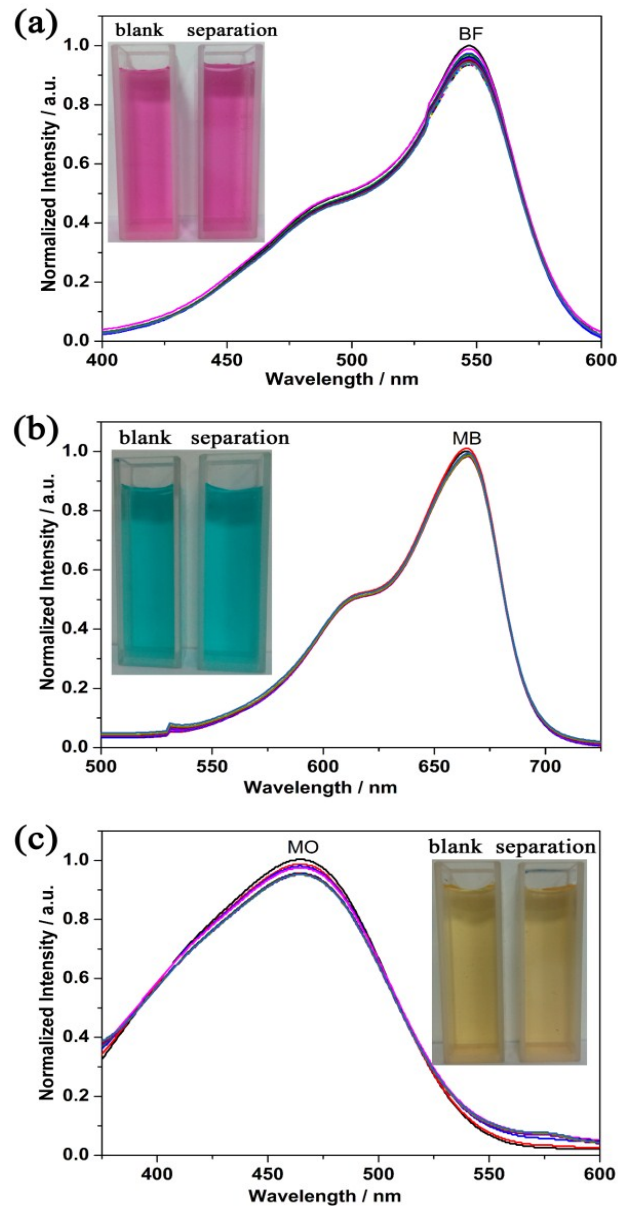


Fig. S18 The UV-vis spectrum of 10^{-5} M dyes filtered with fabricated **HOIFs-1** film by one piece of membrane (filtered for 10 times), the insert is the photograph of the solution for blank and separated solutions (a: BF; b: MB; c: MO).

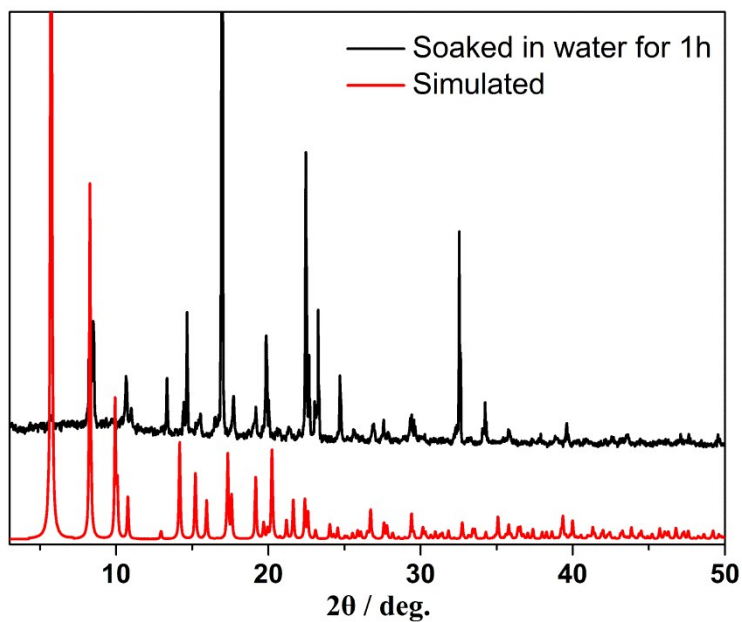


Fig. S19 PXRD comparision of simulated **HOIFs-1** and as-synthesized **HOIFs-1** soaked in water for 1 h.

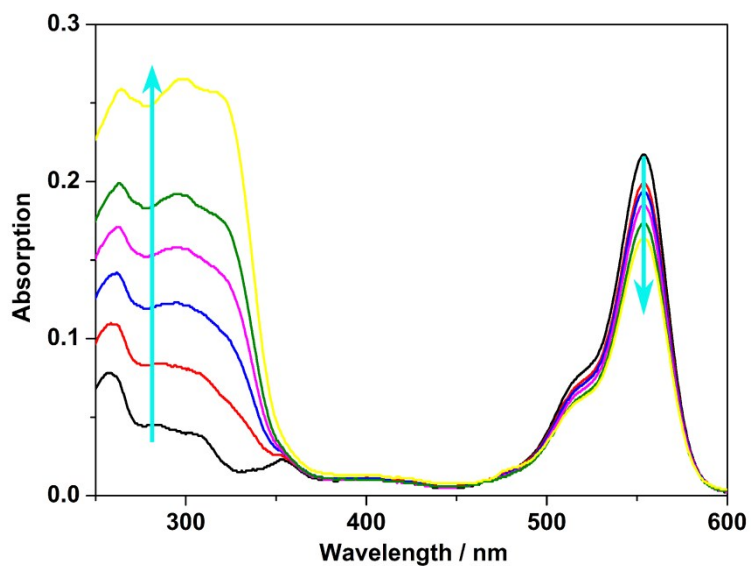


Fig. S20 UV-vis absorption change of the filtrated RhB solution (10^{-5} M), the peak at about 265 nm was ascribed to the UV-vis absorption of $\text{Ln}(\text{NO}_3)_3 \cdot (\text{H}_2\text{O})_3$.

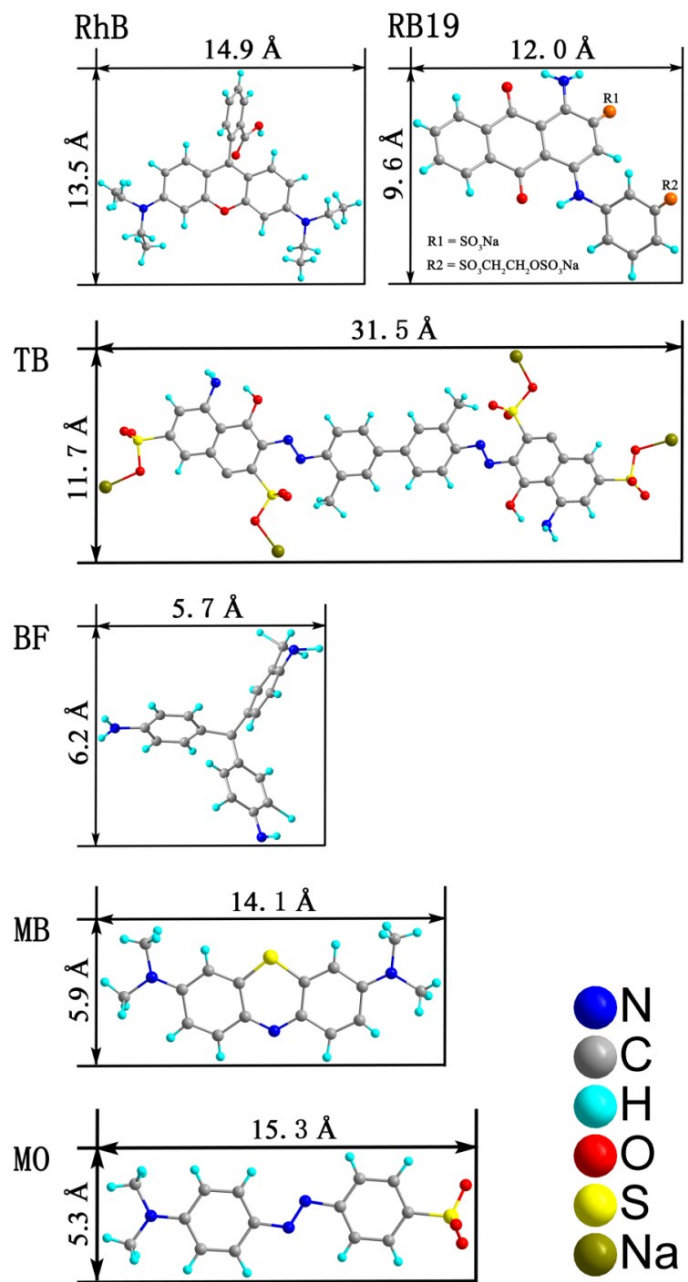


Fig. S21 The sizes of six dyes of RhB, RB 19, TB, BF, MB and MO evaluated by single-crystal data, the two dimension sizes of RhB, RB 19 and TB which can be filtered are larger than 7.5 Å, however, among the dyes of BF, MB and MO, which could not be separated, there is at least one dimension size smaller than 7.5 Å. (7.5 Å is the pore diameter of porous **HOIFs-1**).

Table S1 Crystallographic data and structure refinement parameters for HOIFs **1-3**.

Complex	HOIFs-1	HOIFs-2	HOIFs-3
Empirical formula	Tb ₂ C ₇₂ H ₆₀ N ₂₄ O ₂₄	Er ₂ C ₇₂ H ₆₀ N ₂₄ O ₂₄	Y ₂ C ₇₂ H ₆₀ N ₂₄ O ₂₄
Formula weight	1963.28	1979.96	1823.26
Temperature / K	296(2)	296(2)	293(2)
Wavelength / Å	0.71073	0.71073	0.71073
Crystal system	Triclinic	Triclinic	Triclinic
Space group	P-3c1	P-3c1	P-3c1
a / Å	17.788(3)	17.786(3)	17.694(3)
b / Å	17.788(3)	17.786(3)	17.694(3)
c / Å	21.332(4)	21.419(4)	21.240(4)
α / (°)	90	90	90
β / (°)	90	90	90
γ / (°)	120	120	120
V / Å ³	5845.5(17)	5868.1(17)	5758.8(16)
Z	2	2	2
Calculated density/mg·m ⁻³	1.115	1.121	1.051
Absorption coefficient / mm ⁻¹	1.263	1.483	1.067
F(000)	1964	1976	1860
Crystal size/mm	0.49×0.32×0.23	0.32×0.31×0.21	0.37×0.22×0.12
Theta range for data collection / (°)	1.32 to 25.00	2.32 to 27.43	1.33 to 27.45
Limiting indices	-18 ≤ h ≤ 0, 0 ≤ k ≤ 21, 0 ≤ l ≤ 25	-19 ≤ h ≤ 0, 0 ≤ k ≤ 23, 0 ≤ l ≤ 27	-22 ≤ h ≤ 18, -17 ≤ k ≤ 22, -27 ≤ l ≤ 26
Data / restraints / parameters	3392/4/190	4426/4/190	4344/4/190
Goodness-of-fit on F ²	1.035	1.003	1.005
Final R indices [I > 2sigma(I)] ^a	R ₁ = 0.0605, wR ₂ = 0.1654	R ₁ = 0.0594, wR ₂ = 0.1996	R ₁ = 0.1099, wR ₂ = 0.2958
R indices (all data)	R ₁ = 0.0645, wR ₂ = 0.1690	R ₁ = 0.0670, wR ₂ = 0.2076	R ₁ = 0.1451, wR ₂ = 0.3250
CCDC no.	1510308	1510309	1510310

^a $R = \sum ||F_O| - |F_C|| / \sum |F_O|$, $wR = [\sum w(|F_O|^2 - |F_C|^2)^2 / \sum w(|F_O|^2)]^{1/2}$

Table S2 Hydrogen-Bonding Geometry for **HOIFs-1** (Tb).

donor(D)-H···acceptor(A) (Å)	D-H···A (Å)	D-H (Å)	angle of DHA (deg)
C ₉ -H ₉ ···O ₃	2.419	0.930	139.84
O _{1w} -H _{1wa} ···N ₃	1.886	0.865	164.28
O _{1w} -H _{1wb} ···N ₁	1.918	0.854	153.55

Table S3 Hydrogen-Bonding Geometry for **HOIFs-2** (Er).

donor(D)-H···acceptor(A) (Å)	D-H···A (Å)	D-H (Å)	angle of DHA (deg)
C ₉ -H ₉ ···O ₃	2.431	0.931	141.23
O _{1w} -H _{1wb} ···N ₃	1.926	0.845	160.77
O _{1w} -H _{1wa} ···N ₁	1.944	0.854	150.25

Table S4 Hydrogen-Bonding Geometry for **HOIFs-3** (Y).

donor(D)-H···acceptor(A) (Å)	D-H···A (Å)	D-H (Å)	angle of DHA (deg)
C ₄ -H ₄ ···O ₃	2.491	0.930	127.68
O _{1w} -H _{1wa} ···N ₃	2.145	0.867	120.02
O _{1w} -H _{1wb} ···N ₂	1.910	0.844	164.50

Table S5 Hydrogen coordinates ($\times 10^4$) and isotropic displacement parameters ($\text{A}^2 \times 10^3$) for **HOIFs-1** (Tb).

	x	y	z	U(eq)
H(1)	12090	8452	4294	75
H(2)	11106	8883	4108	98
H(3)	9639	7925	4287	99
H(4)	9217	6523	4587	82
H(9)	9633	4050	6610	101
H(12)	7437	4646	6651	65
H(11)	7828	4223	7575	88
H(10)	8844	3819	7524	92
H(1WA)	5360(40)	2990(30)	5450(30)	116
H(1WB)	5110(40)	2199(16)	5210(30)	116

Table S6 Hydrogen coordinates ($\times 10^4$) and isotropic displacement parameters ($\text{A}^2 \times 10^3$) for **HOIFs-2** (Er).

	x	y	z	U(eq)
H(1)	-2129	6309	5712	57
H(2)	-1174	7778	5824	64
H(3)	331	8288	5690	71
H(4)	757	7296	5385	52
H(9)	363	4428	3388	45
H(10)	1115	4995	2467	60
H(11)	2204	6445	2439	59
H(12)	2580	7229	3366	49
H(1WA)	4840(30)	7040(30)	4810(20)	52
H(1WB)	4620(30)	7630(30)	4610(20)	52

Table S7 Hydrogen coordinates ($\times 10^4$) and isotropic displacement parameters ($\text{A}^2 \times 10^3$) for **HOIFs-3 (Y)**.

	x	y	z	U(eq)
H(1)	4645	7181	6685	70
H(2)	4201	6355	7610	100
H(3)	3771	4891	7554	121
H(4)	3843	4269	6559	108
H(9)	3378	2599	5380	103
H(10)	2036	1672	5689	142
H(11)	1038	2122	5881	138
H(12)	1545	3645	5731	110
H(1WA)	2330(50)	5380(70)	5410(40)	151
H(1WB)	3100(40)	5370(70)	5380(40)	151

Table S8 Bond lengths [\AA] and bond angles [deg] for **HOIFs-1** (Tb).

Tb(1)-O(1W)#1	2.328(4)	C(5)-C(4)	1.392(8)
Tb(1)-O(1W)#2	2.328(4)	C(2)-C(1)	1.356(9)
Tb(1)-O(1W)	2.328(4)	C(2)-C(3)	1.382(10)
Tb(1)-O(2)#2	2.428(3)	C(2)-H(2)	0.9300
Tb(1)-O(2)	2.428(4)	C(3)-C(4)	1.360(10)
Tb(1)-O(2)#1	2.428(3)	C(3)-H(3)	0.9300
Tb(1)-O(1)#2	2.472(4)	C(4)-H(4)	0.9300
Tb(1)-O(1)	2.472(4)	C(1)-H(1)	0.9300
Tb(1)-O(1)#1	2.472(4)	O(2)-N(4)	1.270(6)
O(1W)-H(1WB)	0.86(2)	N(4)-O(3)	1.234(6)
O(1W)-H(1WA)	0.85(2)	C(8)-N(3)	1.301(7)
O(1)-N(4)	1.245(6)	C(8)-C(9)	1.390(8)
N(2)-C(7)	1.306(7)	N(3)-C(12)	1.323(6)
N(2)-C(6)	1.317(8)	C(9)-C(10)	1.380(10)
C(6)-C(7)#3	1.450(9)	C(9)-H(9)	0.9300
C(6)-C(5)	1.481(8)	C(12)-C(11)	1.405(9)
C(7)-C(6)#3	1.450(9)	C(12)-H(12)	0.9300
C(7)-C(8)	1.489(8)	C(11)-C(10)	1.313(11)
N(1)-C(1)	1.309(8)	C(11)-H(11)	0.9300
N(1)-C(5)	1.348(6)	C(10)-H(10)	0.9300
Tb(1)-O(1W)#1	2.328(4)	C(4)-H(4)	0.9300
Tb(1)-O(1W)#2	2.328(4)	C(1)-H(1)	0.9300
Tb(1)-O(1W)	2.328(4)	O(2)-N(4)	1.270(6)
Tb(1)-O(2)#2	2.428(3)	N(4)-O(3)	1.234(6)
Tb(1)-O(2)	2.428(4)	C(8)-N(3)	1.301(7)
Tb(1)-O(2)#1	2.428(3)	C(8)-C(9)	1.390(8)
Tb(1)-O(1)#2	2.472(4)	N(3)-C(12)	1.323(6)
Tb(1)-O(1)	2.472(4)	C(9)-C(10)	1.380(10)
Tb(1)-O(1)#1	2.472(4)	C(9)-H(9)	0.9300
O(1W)-H(1WB)	0.86(2)	C(12)-C(11)	1.405(9)
O(1W)-H(1WA)	0.85(2)	C(12)-H(12)	0.9300
O(1)-N(4)	1.245(6)	C(11)-C(10)	1.313(11)
N(2)-C(7)	1.306(7)	C(11)-H(11)	0.9300
N(2)-C(6)	1.317(8)	C(10)-H(10)	0.9300
C(6)-C(7)#3	1.450(9)	N(1)-C(5)	1.348(6)
C(6)-C(5)	1.481(8)	C(5)-C(4)	1.392(8)

C(7)-C(6)#3	1.450(9)	C(2)-C(1)	1.356(9)
C(7)-C(8)	1.489(8)	C(2)-C(3)	1.382(10)
N(1)-C(1)	1.309(8)	C(2)-H(2)	0.9300
C(3)-C(4)	0.9300	C(3)-H(3)	1.360(10)
O(1W)#1-Tb(1)-O(1W)#2	83.30(15)	N(2)-C(7)-C(8)	114.4(5)
O(1W)#1-Tb(1)-O(1W)	83.30(15)	C(6)#3-C(7)-C(8)	125.3(5)
O(1W)#2-Tb(1)-O(1W)	83.30(15)	C(1)-N(1)-C(5)	119.0(5)
O(1W)#1-Tb(1)-O(2)#2	84.87(14)	N(1)-C(5)-C(4)	120.8(6)
O(1W)#2-Tb(1)-O(2)#2	146.12(13)	N(1)-C(5)-C(6)	118.3(5)
O(1W)-Tb(1)-O(2)#2	126.58(13)	C(4)-C(5)-C(6)	120.7(5)
O(1W)#1-Tb(1)-O(2)	126.58(13)	C(1)-C(2)-C(3)	119.7(7)
O(1W)#2-Tb(1)-O(2)	84.87(14)	C(1)-C(2)-H(2)	120.2
O(1W)-Tb(1)-O(2)	146.12(13)	C(3)-C(2)-H(2)	120.2
O(2)#2-Tb(1)-O(2)	77.03(13)	C(4)-C(3)-C(2)	118.2(6)
O(1W)#1-Tb(1)-O(2)#1	146.12(13)	C(4)-C(3)-H(3)	120.9
O(1W)#2-Tb(1)-O(2)#1	126.58(13)	C(2)-C(3)-H(3)	120.9
O(1W)-Tb(1)-O(2)#1	84.87(14)	C(3)-C(4)-C(5)	119.4(6)
O(2)#2-Tb(1)-O(2)#1	77.03(13)	C(3)-C(4)-H(4)	120.3
O(2)-Tb(1)-O(2)#1	77.03(13)	C(5)-C(4)-H(4)	120.3
O(1W)#1-Tb(1)-O(1)#2	74.06(12)	N(1)-C(1)-C(2)	122.7(6)
O(1W)#2-Tb(1)-O(1)#2	149.76(14)	N(1)-C(1)-H(1)	118.6
O(1W)-Tb(1)-O(1)#2	74.51(13)	C(2)-C(1)-H(1)	118.6
O(2)#2-Tb(1)-O(1)#2	52.16(14)	N(4)-O(2)-Tb(1)	95.5(3)
O(2)-Tb(1)-O(1)#2	124.74(13)	O(3)-N(4)-O(1)	123.4(5)
O(2)#1-Tb(1)-O(1)#2	72.20(13)	O(3)-N(4)-O(2)	118.7(5)
O(1W)#1-Tb(1)-O(1)	74.51(13)	O(1)-N(4)-O(2)	117.8(4)
O(1W)#2-Tb(1)-O(1)	74.06(12)	O(3)-N(4)-Tb(1)	171.3(5)
O(1W)-Tb(1)-O(1)	149.76(14)	O(1)-N(4)-Tb(1)	60.0(2)
O(2)#2-Tb(1)-O(1)	72.20(13)	O(2)-N(4)-Tb(1)	58.1(2)
O(2)-Tb(1)-O(1)	52.16(14)	N(3)-C(8)-C(9)	120.6(6)
O(2)#1-Tb(1)-O(1)	124.74(13)	N(3)-C(8)-C(7)	116.4(5)
O(1)#2-Tb(1)-O(1)	117.25(5)	C(9)-C(8)-C(7)	122.9(6)
O(1W)#1-Tb(1)-O(1)#1	149.76(14)	C(8)-N(3)-C(12)	120.0(5)
O(1W)#2-Tb(1)-O(1)#1	74.51(13)	C(10)-C(9)-C(8)	119.1(7)
O(1W)-Tb(1)-O(1)#1	74.06(12)	C(10)-C(9)-H(9)	120.5
O(2)#2-Tb(1)-O(1)#1	124.74(13)	C(8)-C(9)-H(9)	120.5
O(2)-Tb(1)-O(1)#1	72.20(13)	N(3)-C(12)-C(11)	121.8(6)
O(2)#1-Tb(1)-O(1)#1	52.16(14)	N(3)-C(12)-H(12)	119.1

O(1)#2-Tb(1)-O(1)#1	117.25(5)	C(11)-C(12)-H(12)	119.1
O(1)-Tb(1)-O(1)#1	117.25(5)	C(10)-C(11)-C(12)	118.2(6)
N(4)-O(1)-Tb(1)	94.1(3)	C(10)-C(11)-H(11)	120.9
C(7)-N(2)-C(6)	120.5(5)	C(12)-C(11)-H(11)	120.9
N(2)-C(6)-C(7)#3	119.5(5)	C(11)-C(10)-C(9)	120.1(6)
N(2)-C(6)-C(5)	117.6(5)	C(11)-C(10)-H(10)	120.0
C(7)#3-C(6)-C(5)	122.7(5)	C(9)-C(10)-H(10)	120.0
N(2)-C(7)-C(6)#3	120.0(5)		

Symmetry transformations used to generate equivalent atoms: #1 -y+1, x-y, z; #2 -x+y+1, -x+1, z; #3 -x+2,-y+1,-z+1.

Table S9 Bond lengths [Å] and bond angles [deg] for **HOIFs-2** (Er).

Er(1)-O(1W)#1	2.287(4)	N(1)-C(1)	1.327(7)
Er(1)-O(1W)#2	2.287(4)	C(5)-C(4)	1.389(7)
Er(1)-O(1W)	2.287(4)	C(4)-C(3)	1.381(8)
Er(1)-O(1)	2.395(3)	C(4)-H(4)	0.9300
Er(1)-O(1)#2	2.395(3)	C(8)-N(3)	1.344(6)
Er(1)-O(1)#1	2.395(3)	C(8)-C(9)	1.394(7)
Er(1)-O(2)	2.460(4)	N(3)-C(12)	1.315(6)
Er(1)-O(2)#2	2.460(4)	C(1)-C(2)	1.387(8)
Er(1)-O(2)#1	2.460(4)	C(1)-H(1)	0.9300
N(2)-C(6)	1.320(6)	C(9)-C(10)	1.376(8)
N(2)-C(7)	1.352(6)	C(9)-H(9)	0.9300
O(2)-N(4)	1.252(6)	C(12)-C(11)	1.404(8)
C(6)-C(7)#3	1.409(6)	C(12)-H(12)	0.9300
C(6)-C(5)	1.523(7)	C(2)-C(3)	1.416(9)
C(7)-C(6)#3	1.409(6)	C(2)-H(2)	0.9300
C(7)-C(8)	1.489(7)	C(3)-H(3)	0.9300
O(1W)-H(1WA)	0.861(19)	C(11)-C(10)	1.372(10)
O(1W)-H(1WB)	0.854(19)	C(11)-H(11)	0.9300
N(1)-C(5)	1.317(6)	C(10)-H(10)	0.9300
O(1)-N(4)	1.274(5)	O(3)-N(4)	1.222(5)
O(1W)#1-Er(1)-O(1W)#2	82.87(17)	C(5)-N(1)-C(1)	118.1(5)
O(1W)#1-Er(1)-O(1W)	82.87(17)	N(1)-C(5)-C(4)	123.7(5)
O(1W)#2-Er(1)-O(1W)	82.87(17)	N(1)-C(5)-C(6)	117.2(4)
O(1W)#1-Er(1)-O(1)	84.79(14)	C(4)-C(5)-C(6)	119.0(4)
O(1W)#2-Er(1)-O(1)	126.54(12)	C(5)-C(4)-C(3)	118.4(5)

O(1W)-Er(1)-O(1)	146.20(13)	C(5)-C(4)-H(4)	120.8
O(1W)#1-Er(1)-O(1)#2	126.54(12)	C(3)-C(4)-H(4)	120.8
O(1W)#2-Er(1)-O(1)#2	146.20(13)	N(3)-C(8)-C(9)	121.1(5)
O(1W)-Er(1)-O(1)#2	84.79(14)	N(3)-C(8)-C(7)	116.7(4)
O(1)-Er(1)-O(1)#2	77.61(13)	C(9)-C(8)-C(7)	122.0(5)
O(1W)#1-Er(1)-O(1)#1	146.20(13)	C(12)-N(3)-C(8)	118.5(5)
O(1W)#2-Er(1)-O(1)#1	84.79(14)	N(1)-C(1)-C(2)	123.8(6)
O(1W)-Er(1)-O(1)#1	126.54(12)	N(1)-C(1)-H(1)	118.1
O(1)-Er(1)-O(1)#1	77.61(13)	C(2)-C(1)-H(1)	118.1
O(1)#2-Er(1)-O(1)#1	77.61(13)	C(10)-C(9)-C(8)	119.8(5)
O(1W)#1-Er(1)-O(2)	73.99(12)	C(10)-C(9)-H(9)	120.1
O(1W)#2-Er(1)-O(2)	74.26(13)	C(8)-C(9)-H(9)	120.1
O(1W)-Er(1)-O(2)	149.07(15)	N(3)-C(12)-C(11)	123.8(5)
O(1)-Er(1)-O(2)	52.35(13)	N(3)-C(12)-H(12)	118.1
O(1)#2-Er(1)-O(2)	125.51(13)	C(11)-C(12)-H(12)	118.1
O(1)#1-Er(1)-O(2)	72.39(13)	C(1)-C(2)-C(3)	117.4(5)
O(1W)#1-Er(1)-O(2)#2	74.26(13)	C(1)-C(2)-H(2)	121.3
O(1W)#2-Er(1)-O(2)#2	149.07(15)	C(3)-C(2)-H(2)	121.3
O(1W)-Er(1)-O(2)#2	73.99(12)	C(4)-C(3)-C(2)	118.5(5)
O(1)-Er(1)-O(2)#2	72.39(13)	C(4)-C(3)-H(3)	120.7
O(1)#2-Er(1)-O(2)#2	52.35(13)	C(2)-C(3)-H(3)	120.7
O(1)#1-Er(1)-O(2)#2	125.51(13)	C(10)-C(11)-C(12)	117.6(5)
O(2)-Er(1)-O(2)#2	117.47(5)	C(9)-C(10)-C(11)	119.1(5)
O(1W)#1-Er(1)-O(2)#1	149.07(15)	C(9)-C(10)-H(10)	120.4
O(1W)#2-Er(1)-O(2)#1	73.99(12)	C(11)-C(10)-H(10)	120.4
O(1W)-Er(1)-O(2)#1	74.26(13)	N(4)-O(1)-Er(1)	96.8(3)
O(1)-Er(1)-O(2)#1	125.51(13)	O(3)-N(4)-O(2)	123.2(4)
O(1)#2-Er(1)-O(2)#1	72.39(13)	O(3)-N(4)-O(1)	120.8(4)
O(1)#1-Er(1)-O(2)#1	52.35(13)	O(2)-N(4)-O(1)	116.0(4)
O(2)-Er(1)-O(2)#1	117.47(5)	O(3)-N(4)-Er(1)	171.8(4)
O(2)#2-Er(1)-O(2)#1	117.47(5)	O(2)-N(4)-Er(1)	59.6(2)
C(6)-N(2)-C(7)	118.0(4)	O(1)-N(4)-Er(1)	56.8(2)
N(4)-O(2)-Er(1)	94.3(3)	N(2)-C(7)-C(8)	112.8(4)
N(2)-C(6)-C(7)#3	122.5(4)	C(6)#3-C(7)-C(8)	127.6(4)
N(2)-C(6)-C(5)	115.3(4)	Er(1)-O(1W)-H(1WA)	127(2)
C(7)#3-C(6)-C(5)	122.0(4)	Er(1)-O(1W)-H(1WB)	127(3)
N(2)-C(7)-C(6)#3	119.5(5)	H(1WA)-O(1W)-	106(4)
		H(1WB)	

Symmetry transformations used to generate equivalent atoms: #1 -y+1, x-y+1, z; #2 -x+y, -x+1, z; #3 -x, -y+1, -z+1.

Table S10 Bond lengths [Å] and bond angles [deg] for **HOIFs-3 (Y)**.

Y(1)-O(1W)#1	2.300(5)	N(4)-C(6)#3	1.506(10)
Y(1)-O(1W)#2	2.300(5)	C(9)-C(10)	1.302(15)
Y(1)-O(1W)	2.300(5)	C(9)-C(8)	1.427(11)
Y(1)-O(2)#2	2.401(4)	C(9)-H(9)	0.9300
Y(1)-O(2)#1	2.401(4)	O(3)-N(1)	1.233(9)
Y(1)-O(2)	2.401(4)	C(5)-C(4)	1.397(11)
Y(1)-O(1)#1	2.439(5)	C(5)-C(6)	1.540(10)
Y(1)-O(1)#2	2.439(5)	C(12)-C(11)	1.476(14)
Y(1)-O(1)	2.439(5)	C(12)-H(12)	0.9300
O(2)-N(1)	1.198(7)	C(6)-C(7)	1.242(12)
O(1)-N(1)	1.398(8)	C(6)-N(4)#3	1.506(10)
O(1W)-H(1WB)	0.86(2)	C(10)-C(11)	1.354(16)
O(1W)-H(1WA)	0.84(2)	C(10)-H(10)	0.9300
N(2)-C(5)	1.318(9)	C(8)-C(7)	1.552(13)
N(2)-C(1)	1.315(8)	C(2)-C(3)	1.368(14)
C(1)-C(2)	1.412(11)	C(2)-H(2)	0.9300
C(1)-H(1)	0.9300	C(4)-C(3)	1.446(12)
N(3)-C(12)	1.237(11)	C(4)-H(4)	0.9300
N(3)-C(8)	1.432(10)	C(11)-H(11)	0.9300
N(4)-C(7)	1.326(11)	C(3)-H(3)	0.9300
O(1W)#1-Y(1)-O(1W)#2	83.81(19)	N(2)-C(1)-H(1)	118.6
O(1W)#1-Y(1)-O(1W)	83.81(19)	C(2)-C(1)-H(1)	118.6
O(1W)#2-Y(1)-O(1W)	83.81(19)	C(12)-N(3)-C(8)	117.2(7)
O(1W)#1-Y(1)-O(2)#2	84.49(16)	C(7)-N(4)-C(6)#3	111.7(6)
O(1W)#2-Y(1)-O(2)#2	127.50(15)	C(10)-C(9)-C(8)	121.4(8)
O(1W)-Y(1)-O(2)#2	144.90(15)	C(10)-C(9)-H(9)	119.3
O(1W)#1-Y(1)-O(2)#1	127.50(15)	C(8)-C(9)-H(9)	119.3
O(1W)#2-Y(1)-O(2)#1	144.90(15)	O(2)-N(1)-O(3)	124.2(7)
O(1W)-Y(1)-O(2)#1	84.49(16)	O(2)-N(1)-O(1)	118.1(6)
O(2)#2-Y(1)-O(2)#1	76.78(15)	O(3)-N(1)-O(1)	117.6(7)
O(1W)#1-Y(1)-O(2)	144.90(15)	O(2)-N(1)-Y(1)	58.6(3)
O(1W)#2-Y(1)-O(2)	84.49(16)	O(3)-N(1)-Y(1)	172.8(5)
O(1W)-Y(1)-O(2)	127.50(15)	O(1)-N(1)-Y(1)	60.6(3)

O(2)#2-Y(1)-O(2)	76.78(15)	N(2)-C(5)-C(4)	125.4(7)
O(2)#1-Y(1)-O(2)	76.78(15)	N(2)-C(5)-C(6)	118.3(6)
O(1W)#1-Y(1)-O(1)#1	72.69(18)	C(4)-C(5)-C(6)	116.1(7)
O(1W)#2-Y(1)-O(1)#1	149.84(19)	N(3)-C(12)-C(11)	126.5(9)
O(1W)-Y(1)-O(1)#1	75.25(16)	N(3)-C(12)-H(12)	116.7
O(2)#2-Y(1)-O(1)#1	69.69(17)	C(11)-C(12)-H(12)	116.7
O(2)#1-Y(1)-O(1)#1	54.83(17)	C(7)-C(6)-N(4)#3	119.2(7)
O(2)-Y(1)-O(1)#1	125.52(17)	C(7)-C(6)-C(5)	134.7(8)
O(1W)#1-Y(1)-O(1)#2	75.25(16)	N(4)#3-C(6)-C(5)	105.8(6)
O(1W)#2-Y(1)-O(1)#2	72.69(18)	C(9)-C(10)-C(11)	122.3(11)
O(1W)-Y(1)-O(1)#2	149.84(19)	C(9)-C(10)-H(10)	118.8
O(2)#2-Y(1)-O(1)#2	54.83(17)	C(11)-C(10)-H(10)	118.9
O(2)#1-Y(1)-O(1)#2	125.52(17)	C(9)-C(8)-N(3)	117.8(7)
O(2)-Y(1)-O(1)#2	69.69(17)	C(9)-C(8)-C(7)	124.8(7)
O(1)#1-Y(1)-O(1)#2	117.38(7)	N(3)-C(8)-C(7)	117.0(6)
O(1W)#1-Y(1)-O(1)	149.84(19)	C(6)-C(7)-N(4)	129.1(9)
O(1W)#2-Y(1)-O(1)	75.25(16)	C(6)-C(7)-C(8)	119.2(8)
O(1W)-Y(1)-O(1)	72.70(17)	N(4)-C(7)-C(8)	111.4(8)
O(2)#2-Y(1)-O(1)	125.52(17)	C(3)-C(2)-C(1)	117.8(8)
O(2)#1-Y(1)-O(1)	69.69(17)	C(3)-C(2)-H(2)	121.1
O(2)-Y(1)-O(1)	54.83(17)	C(1)-C(2)-H(2)	121.1
O(1)#1-Y(1)-O(1)	117.38(7)	C(5)-C(4)-C(3)	113.8(9)
O(1)#2-Y(1)-O(1)	117.38(7)	C(5)-C(4)-H(4)	123.1
N(1)-O(2)-Y(1)	96.2(4)	C(3)-C(4)-H(4)	123.1
N(1)-O(1)-Y(1)	89.4(4)	C(10)-C(11)-C(12)	114.4(11)
Y(1)-O(1W)-H(1WB)	121(4)	C(10)-C(11)-H(11)	122.8
Y(1)-O(1W)-H(1WA)	123(5)	C(12)-C(11)-H(11)	122.8
H(1WB)-O(1W)-	107(5)	C(2)-C(3)-C(4)	120.7(9)
H(1WA)	118.6(6)	C(2)-C(3)-H(3)	119.7
C(5)-N(2)-C(1)	122.8(7)	C(4)-C(3)-H(3)	119.7
N(2)-C(1)-C(2)			

Symmetry transformations used to generate equivalent atoms: #1 -x+y,-x+1,z; #2 -y+1,x-y+1,z; #3 -x+1,-y+1,-z+1.

Table S11 Atomic coordinates ($\times 10^4$) and equivalent isotropic displacement parameters ($\text{Å}^2 \times 10^3$) for **HOIFs-1** (Tb). U(eq) is defined as one third of the trace of the orthogonalized U_{ij} tensor.

	x	y	z	U(eq)
Tb(1)	4475(1)	6667	3333	36(1)
O(1W)	5507(3)	2739(2)	5175(2)	46(1)
O(1)	8248(3)	4152(3)	4281(2)	56(1)
N(2)	9675(2)	5476(3)	5277(2)	48(1)
C(6)	10179(3)	5785(4)	4781(3)	55(1)
C(7)	9480(4)	4721(4)	5508(3)	51(1)
N(1)	11273(3)	7252(3)	4492(2)	57(1)
C(5)	10423(3)	6672(4)	4570(2)	51(1)
C(2)	10919(5)	8319(5)	4240(4)	82(2)
C(3)	10046(5)	7748(6)	4338(4)	82(2)
C(4)	9798(4)	6920(5)	4510(3)	68(2)
C(1)	11503(4)	8051(5)	4338(3)	62(2)
O(2)	7445(2)	4436(2)	3684(2)	50(1)
N(4)	8197(3)	4613(3)	3863(2)	53(1)
O(3)	8835(3)	5249(4)	3633(2)	96(2)
C(8)	8972(4)	4493(3)	6101(3)	52(1)
N(3)	8326(3)	4641(3)	6117(2)	46(1)
C(9)	9185(4)	4176(6)	6627(3)	84(3)
C(12)	7895(3)	4535(3)	6646(2)	54(1)
C(11)	8111(5)	4258(5)	7200(3)	73(2)
C(10)	8723(4)	4050(6)	7174(3)	77(2)

Table S12 Atomic coordinates ($\times 10^4$) and equivalent isotropic displacement parameters ($\text{Å}^2 \times 10^3$) for **HOIFs-2** (Er). U(eq) is defined as one third of the trace of the orthogonalized U_{ij} tensor.

	x	y	z	U(eq)
Er(1)	3333	6667	5544(1)	31(1)
N(2)	321(2)	5811(3)	4721(2)	31(1)
O(2)	1758(3)	5922(2)	5729(2)	43(1)
C(6)	-187(3)	5590(3)	5217(2)	32(1)
C(7)	517(3)	5223(3)	4489(2)	31(1)
O(1W)	4468(3)	7206(2)	4855(2)	40(1)
N(1)	-1289(2)	5951(3)	5503(2)	38(1)
C(5)	-455(3)	6245(3)	5417(2)	33(1)
C(4)	177(3)	7115(3)	5465(3)	44(1)
C(8)	1036(3)	5522(3)	3903(2)	35(1)
N(3)	1700(2)	6345(3)	3896(2)	34(1)
C(1)	-1540(4)	6517(4)	5652(3)	48(1)
C(9)	812(3)	5002(3)	3372(2)	38(1)
C(12)	2119(3)	6661(3)	3368(2)	41(1)
C(2)	-973(4)	7400(4)	5723(3)	53(1)
C(3)	-77(4)	7704(4)	5635(3)	59(2)
C(11)	1910(4)	6190(5)	2807(2)	49(1)
C(10)	1256(4)	5339(4)	2823(3)	50(1)
O(1)	2572(2)	7003(3)	6316(2)	38(1)
O(3)	1173(3)	6439(3)	6364(2)	61(1)
N(4)	1807(2)	6441(3)	6144(2)	35(1)

Table S13 Atomic coordinates ($\times 10^4$) and equivalent isotropic displacement parameters ($\text{Å}^2 \times 10^3$) for **HOIFs-3** (Y). U(eq) is defined as one third of the trace of the orthogonalized U_{ij} tensor.

	x	y	z	U(eq)
Y(1)	3333	6667	4489(1)	43(1)
O(2)	4432(3)	7010(3)	3701(2)	52(1)
O(1)	4084(4)	5848(4)	4301(3)	78(2)
O(1W)	2762(3)	5509(3)	5178(2)	60(1)
N(2)	4614(3)	6286(4)	6139(2)	56(1)
C(1)	4517(4)	6603(5)	6674(3)	59(2)
N(3)	2687(5)	4006(4)	5506(3)	81(2)
N(4)	4495(4)	4176(4)	4711(3)	66(2)
C(9)	3000(7)	2807(6)	5473(4)	86(2)
O(3)	5252(5)	6436(5)	3658(3)	109(2)
N(1)	4628(5)	6484(5)	3869(3)	76(2)
C(5)	4445(5)	5471(5)	6126(3)	72(2)
C(12)	1938(7)	3450(7)	5664(5)	92(3)
C(6)	4622(5)	5123(5)	5512(3)	63(2)
C(10)	2203(9)	2258(8)	5643(6)	118(4)
C(8)	3308(5)	3719(5)	5425(3)	67(2)
C(7)	4245(7)	4418(7)	5224(5)	90(3)
C(2)	4226(6)	6104(7)	7232(4)	84(2)
C(4)	4047(7)	4862(7)	6610(4)	90(3)
C(11)	1608(9)	2510(8)	5756(5)	115(4)
C(3)	3982(8)	5240(8)	7197(4)	101(3)

Table S14 Experimental IR and Raman peaks comparison and peaks assignment for TPPZ and **HOIFs-1**. Note: vs = very strong; s = strong; m = medium; w = weak.

IR peaks / cm ⁻¹		Raman peaks / cm ⁻¹		Assignments
TPPZ	HOIFs-1	TPPZ	HOIFs-1	
3049(m)	3057(vs)	3150(w)	3166(m)	C-H stretching
—	3021(vs)	—	3033(m)	Symmetric stretching
—	—	3054(m)	3084(w)	C-H stretching
—	—	—	3030(w)	C-H stretching
—	1704(w)	2987	2980(w)	O-H scissoring
—	—	2937	2936(w)	O-H stretching
1587(vs)	1593(vs)	1642(vs)	1646(vs)	Pyridine ring deformation
1566(vs)	1568(s)	1616(m)	1620(m)	Pyrazine ring deformation
1485(w)	1481(vs)	1576(vs)	1584(vs)	C=C strectching of pyrazine ring
1435(m)	—	1518(w)	1521(w)	C-C strectching, C-H rocking, N=O stretching
1393(vs)	1394(s)	1489(m)	1481(m)	C-H rocking
1286(w)	1286(vs)	1378(vs)	1376(vs)	Pyrazine ring deformation
1238(w)	—	1316(m)	1316(m)	C=N stretching of pyrazine ring
1227(w)	—	1278(m)	1286(m)	C=N stretching of pyrazine ring
1150(m)	1151(s)	1189(w)	1191(w)	C=C stretching, O-N-O bending
1124(vs)	—	1135(w)	1133(w)	C-H wagging
1094(m)	—	1105(w)	1107(w)	C-C=C bending
1061(w)	1061(m)	1073(m)	1075(w)	C-N=C bending
1036(s)	1030(s)	—	1065(m)	C-H twisting
989(m)	1005(s)	1022(s)	1035(s)	Pyridine ring deformation
901(w)	901(w)	930(w)	944(w)	C-H wagging
—	899(w)	—	900(w)	N=O stretching
806(s)	810(m)	866(w)	864(w)	C-H wagging, C=C bending
785(vs)	785(s)	837(w)	836(w)	C-C=C bending, C-H wagging
754(vs)	741(s)	777(w)	767(w)	C-C=C bending
716(w)	700(w)	743(m)	743(m)	Ring deformation
—	—	—	705(w)	O-H wagging
625(w)	631(w)	683(w)	679(w)	Pyridine ring deformation
552(s)	554(s)	592(w)	592(w)	C-N=C bending
503(w)	507(w)	530(w)	530(w)	C=N stretching of pyridine ring
407(m)	407(w)	423(m)	421(w)	N-C=C bending, C-H twisting